Geophysical Journal International

Geophys. J. Int. (2011) **187,** 946–958 doi: 10.1111/j.1365-246X.2011.05194.x

AusMoho: the variation of Moho depth in Australia

B. L. N. Kennett, M. Salmon, E. Saygin and AusMoho Working Group*

Research School of Earth Sciences, The Australian National University, Canberra ACT 0200*, Australia. E-mail: Brian.Kennett@anu.edu.au*

Accepted 2011 August 15. Received 2011 August 12; in original form 2011 March 9

SUMMARY

Since 2004 more than 7000 km of full-crustal reflection profiles have been collected across Australia to give a total of more than 11 000 km, providing valuable new constraints on crustal structure. A further set of hitherto unexploited results comes from 150 receiver functions distributed across the continent, mostly from portable receiver sites. These new data sets provide a dramatic increase in data coverage compared with previous studies, and reveal the complex structure of the Australian continent in considerable detail.

A new comprehensive model for Moho depth across Australia and its immediate environment is developed by utilizing multiple sources of information. On-shore and off-shore refraction experiments are supplemented by receiver functions from a large number of portable stations and the recently augmented set of permanent stations, and Moho picks from the full suite of reflection transects. The composite data set provides a much denser sampler of most of the continent than before, though coverage remains low in the remote areas of the Simpson and Great Sandy deserts. The various data sets provide multiple estimates of the depth to Moho in many regions and the consistency between the different techniques is high. In a number of instances, differences in estimates of Moho depth can be associated with the aspects of the structure highlighted by the particular methods.

The new results allow considerable refinement of the patterns of Moho depth across the continent. Some of the thinnest crust lies beneath the Archean cratons in the Pilbara and the southern part of the Yilgarn. Thick crust is encountered beneath parts of the Proterozoic in Central Australia, and beneath the Palaeozoic Lachlan fold belt in southeastern Australia. The refined data indicate a number of zones of sharp contrast in depth to Moho, notably in the southern part of Central Australia.

Key words: Controlled source seismology; Broad-band seismometers; Body waves; Australia.

GJI Seismology

1 INTRODUCTION

In the 100 yr since the detection of the base of the crust by Mohorovičić (1910) from a limited number of observations of earthquakes in Croatia, the discontinuity bearing his name has been recognized as an ubiquitous feature in both continental and oceanic domains. Though the character of the transition from crust to mantle can vary from sharp to highly gradational, the 'Moho' represents a distinct change in physical properties linked to the change in chemical constituents between crust and mantle. Information on the Moho beneath Australia has progressively been developed through the combination of refraction, reflection and receiver function studies. Since the mean elevation of Australia is only 325 m, in most places the distinction between the depth to Moho and the crustal thickness is small, and probably within the error of estimates. Nevertheless there are a few places across the continent where the differences could matter and so we work throughout in terms of Moho depth.

Australia has a long and complex tectonic history. The Australian continental crust was accreted in three major episodes, each comprising about one third of the continental area from the Archean cratons in the west to Phanerozoic provinces in the east. Disparate Archean crustal elements were assembled into three major cratonic zones in the Proterozoic; West Australia, the North Australian Craton and the South Australian Craton were formed by 1830 Ma, and these cratonic elements were joined to the Rodinian supercontinent by 1300–1100 Ma (Cawood & Korsch 2008). The supercontinent broke up around 800 Ma. Subsequently, the fold belt structures of the Phanerozoic Tasman Orogen of the eastern third of Australia were accreted onto the eastern margin of the Precambrian cratons in the late Palaeozoic in a series of stages (e.g. Direen & Crawford 2003). In the Mesozoic, Australia was the continental margin of the subducting Pacific Plate and subsequently a chain of

*In addition to the principal authors the AusMoho Working Group comprises: N. Rawlinson, S. Pozgay, H. Tkalčić, E. Vanacore, The Australian National University; C. Collins, B. Goleby, A. Goncharov, J. Maher, Geoscience Australia; A.M. Reading, University of Tasmania; A. Aitken, S. Revets, University of Western Australia; T. Shibutani, Kyoto University; G. Clitheroe, GNS, New Zealand; P. Arroucau, North Carolina Central University, F.R. Fontaine, Université de Reunion.

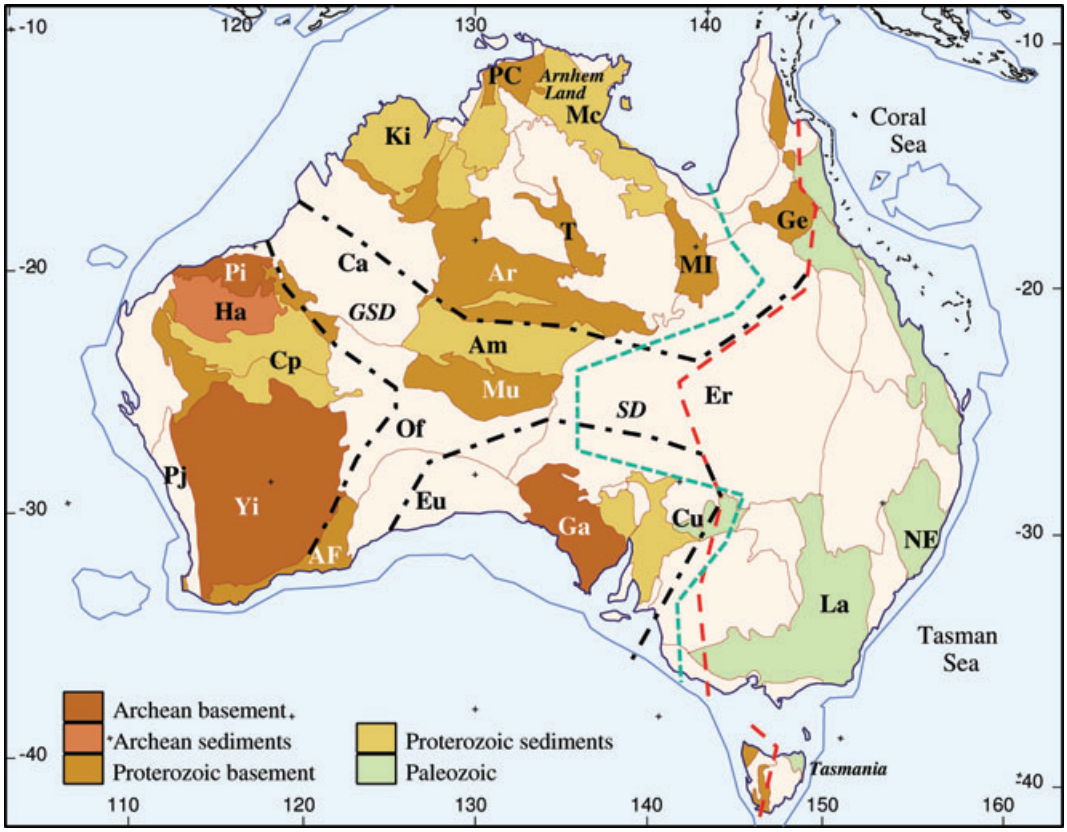

Figure 1. Simplified representation of the main tectonic features of Australia. The outline of the major cratons are marked by chain-dotted lines. The Tasman line in red is based on the reinterpretation by Direen & Crawford (2003). The cyan dashed line indicates the eastern boundary of the main block of thickened crust. Key to marked features: AF, Albany-Fraser belt; Ar, Arunta Block; Am, Amadeus Basin; Ca, Canning Basin; Cp, Capricorn Orogen; Cu, Curnamona Craton; Er, Eromanga Basin; Eu, Eucla Basin, Ga, Gawler Craton; Ge, Georgetown inlier; Ha, Hamersley Basin; Ki, Kimberley Block; La, Lachlan Orogen; Mc, MacArthur Basin; MI, Mt Isa Block; Mu, Musgrave Block; NE, New England Orogen; Of, Officer Basin; PC, Pine Creek Inlier; Pi, Pilbara Craton; Pj, Pinjarra Orogen; T, Tennant Creek Block; Yi, Yilgarn Craton; SD, Simpson Desert; GSD, Great Sandy Desert.

hotspot-related volcanism has developed through eastern Australia. The eastern margin of Australia has been influenced by seafloor spreading in the Tasman Sea from 80 Ma and backarc spreading in the Coral Sea. Around 80 per cent of Australia is covered by extensive Mesozoic and younger sedimentary rocks and thick regolith, so that outcrop is limited. In Fig. 1 we show a simplified model of the tectonics of Australia, with an indication of the age of the major elements. The areas in beige have extensive regolith cover with very little outcrop. We also indicate the cratonic boundaries based on the work of Cawood & Korsch (2008), and the Tasman line based on the reinterpretation by Direen & Crawford (2003).

The original concept of the Tasman line was based on the easternmost outcrop of the Precambrian material, but such outcrop is limited along much of the length. Many different interpretations have been invoked based on lineations derived from potential field measurements (gravity and magnetics) that are likely to arise from features in the upper part of the crust. The Tasman line has been related to the edge of the continent at the time of breakup of Rodinia, but in the mantle, the main contrasts lie somewhat to the east (Kennett *et al.* 2004; Fishwick *et al.* 2008). Recent crustal reflection surveys in South Australia and western Victoria support the location indicated in Fig. 1, that links to changes at the base of the crust. In Fig. 1 we also display, as a cyan dashed line, the general outline of the eastern edge of thickened crust based on the study later. This outline has a general correspondence to the Tasman line, but displays a strong embayment into central Australia that might be linked to a zone of slightly thinner lithosphere within the thick cratonic zone (Fishwick *et al.* 2008).

Collins (1991) presented a compilation of refraction results across the Australian continent to provide the first general outlines of Moho depth. The major features of the pattern of Moho depth began to appear in the study by Clitheroe *et al.* (2009), which included information from 65 receiver function studies, mostly from portable broad-band stations, in addition to the 51 estimates employed by Collins, and produced a continent wide map of Moho depth. Collins *et al.* (2003) added Moho depth information from off-shore refraction work to extend the Moho depth patterns out to the oceanic domains. Some further data from marine sources was included in the study by Goncharov *et al.* (2007).

This group of studies provides sparse, irregular, coverage of the Australian continent with a typical separation of sample points of 150–250 km. The pattern of Moho depth shows thick crust (more than 50 km thick) beneath the Proterozoic part of the North Australia craton, localized thickened crust in southwestern Australia, and a prominent zone with a thick gradational base to the crust beneath the southern part of the Lachlan fold belt in eastern Australia. Fig. 2 illustrates these Moho depth patterns using the same interpolation and colour scheme as is subsequently employed for the new, more extensive data set. The locations of the sample points

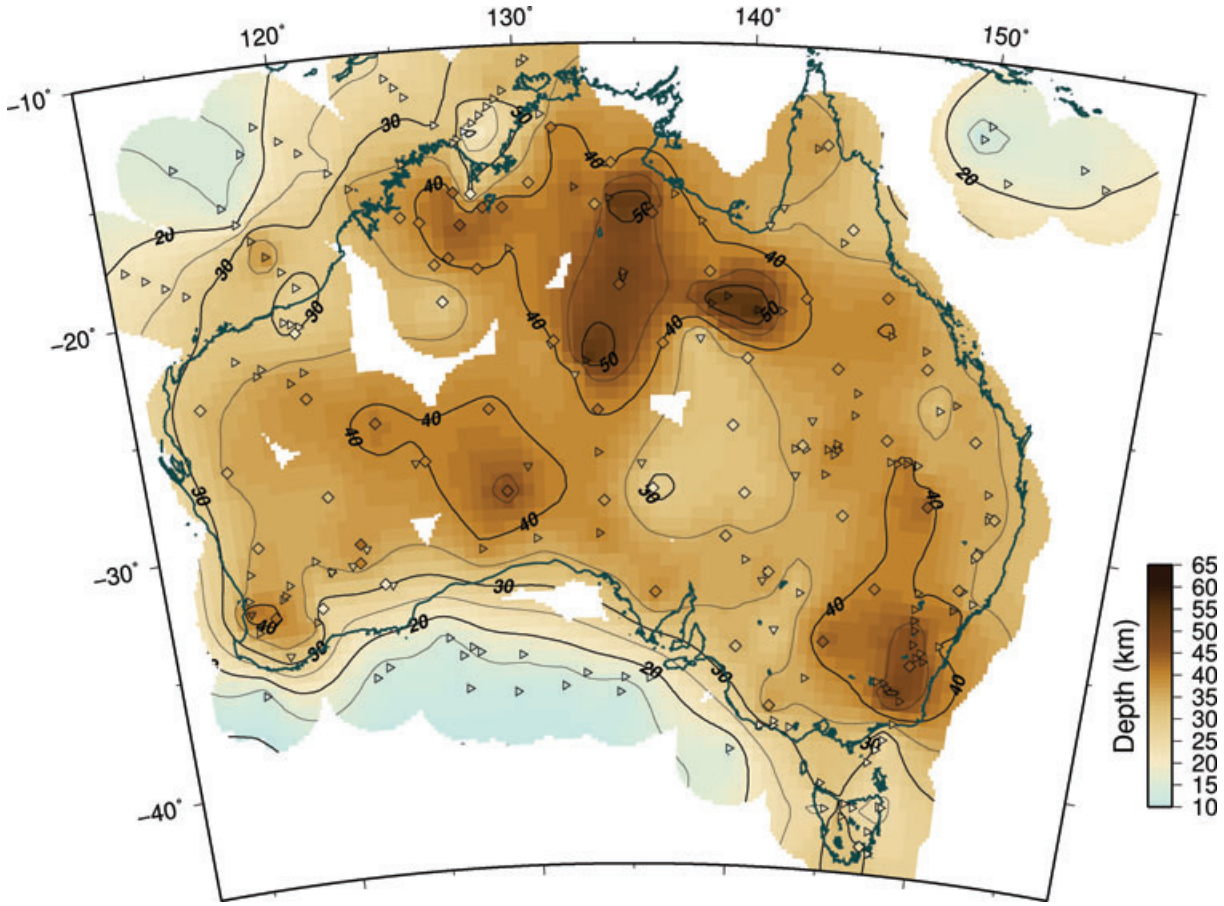

Figure 2. Moho surface constructed from the results reported by Collins *et al.* (2003), using the same procedure as for the new compilation (see Fig. 4). Results from refraction experiments are indicated by triangles, receiver function results by diamonds and data from historic reflection work by inverted triangles. The Moho estimates at each point are indicated with the same colour code as the interpolated surface, shown at the right with depths in kilometres. A mask of radius 250 km is applied around each data point, so that areas with poor constraint can be identified.

are superimposed on the interpolated surface with the colour code associated with the data value.

A continuing campaign of broad-band deployments across the continent (see, e.g. Kennett 2003) has seen a large number of broad-band portable stations installed. Receiver function analysis has now been carried out for most of these stations. Recently dense arrays of three-component short-period instruments have been deployed in southeastern Australia (Rawlinson *et al.* 2011), and the data have been used to construct receiver functions using higher frequency data. More than 150 new receiver function sites are available from these sources and have been used to augment the database for Moho depths. A particular focus of the portable deployments since 2000 has been on western Australia with a number of deployments that now provide good coverage of the Archean cratons and the Proterozoic Capricorn orogen. The receiver function studies have provided clear evidence for segmentation of the Yilgarn cratons with characteristic crustal structures for the individual terranes (Reading *et al.* 2007).

A further major data source comes from more than 11 000 km of full-crustal reflection profiles that have been conducted since the late 1970s in many parts of the Australian continent. The transects mostly carried out by Geoscience Australia and its predecessors, have targeted different aspects of crustal structure in Archean, Proterozoic and Phanerozoic terranes. Often the profiles have been conducted to provide new information in areas of economic interest or where there may be economic potential. Moho depth estimates extracted from the record sections at 20–40 km intervals help to link the spatially distinct sampling from the other techniques.

2 DATA SOURCES

The different sources of information on Moho depth from seismological studies are shown in Figs 3(a)–(c), with a common colour scale for the depth to Moho. The size of the symbols provide an indication of the confidence to be placed in the results; larger symbols signify the best constrained results.

For consistency with earlier results we have employed a definition for the base of the crust such that the Moho is taken as the boundary where the velocities on the lower side are greater than 7.8 km s^{-1} for *P* waves and 4.4 km s^{-1} for shear waves. Where the transition from crust to mantle occurs through a velocity gradient we take the base of the transition. Clitheroe *et al.* (2009) discuss the relationship of this style of definition for Moho depth to estimates based on changes in petrology in xenoliths for the Lachlan fold belt in eastern Australia (O'Reilly & Griffin 1996). Once the uncertainties in each approach are recognized the results are broadly consistent, but the two approaches to the definition of the base of the crust can be

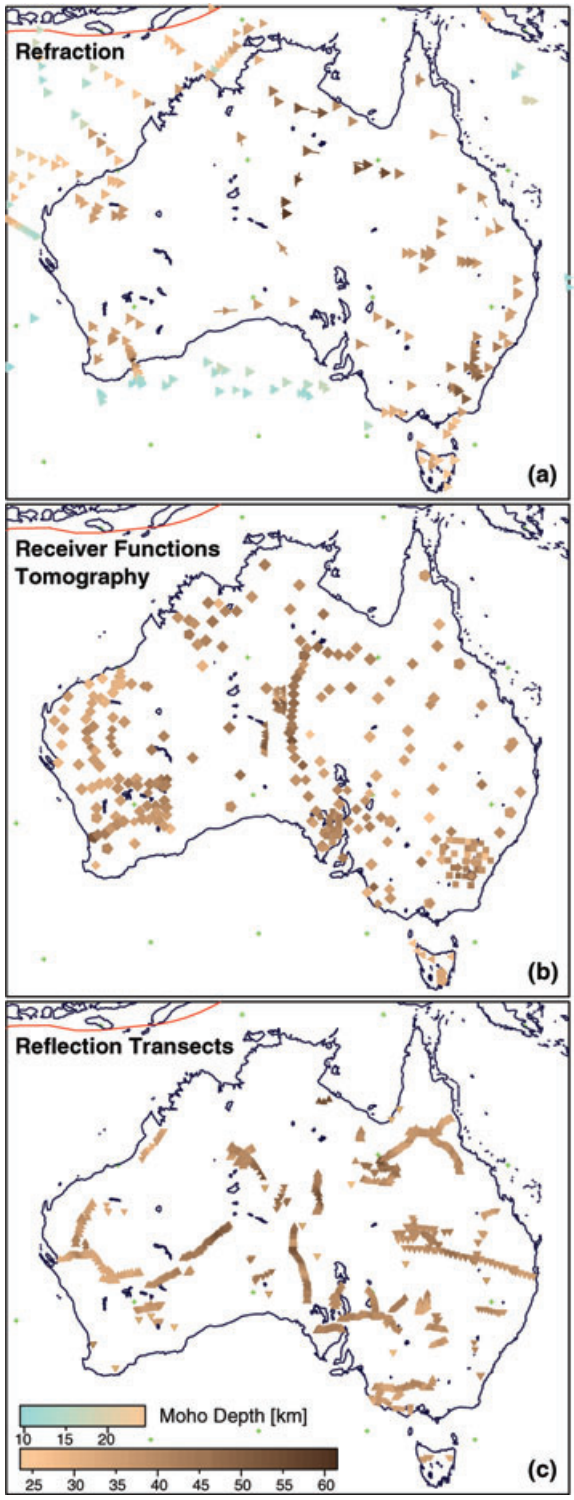

Figure 3. The set of Moho depth estimates used in the construction of the new Moho surface: (a) refraction experiments, (b) receiver functions and tomographic results, (c) reflection transects and results from early short reflection surveys. In all panels the size of symbols increases with the reliability of the results.

expected to emphasize different aspects of a broad Moho transition zone.

We summarize the sources of information on Moho depth employed in this study in Table 1.

2.1 Refraction data

The refraction results (Fig. 3a) are taken from the compilation by Collins *et al.* (2003) with some supplements for offshore–onshore work in western Australia from Goncharov *et al.* (2007) Moho estimates from refraction work are not point results and as the density of other information increases we need to be more careful with placement. In many cases we have therefore used line indicators for the direction of the survey and the likely zone of sampling. Such information becomes important where, as in central Australia, there is a strong grain to structure with major east–west features in the gravity field linked to significant topography on the crust–mantle boundary (Goleby *et al.* 1989; Aitken 2010). Most on-shore refraction surveys date from the 1960s to 1980s and there has been little such work since, except off-shore/on-shore experiments mostly in western Australia.

2.2 Receiver functions

Most of the receiver function studies (Fig. 3b) have been carried out using waveform matching methods for broad-band stations. Shibutani *et al.* (1996) made use of genetic algorithm inversion for waveform fitting of receiver functions to generate 1-D shear wave speed and V_p/V_s profiles for portable stations in eastern Australia. This work was extended by Clitheroe *et al.* (2009) to cover most of the continent through the portable stations of the SKIPPY experiment (van der Hilst *et al.* 1994), and the limited number of high-quality permanent stations at the time. Subsequent inversions have employed the Neighbourhood Algorithm of Sambridge (1999) for the waveform fits. A set of such studies have been made of the West Australian cratons as detailed coverage has become available through portable broad-band deployments (Reading & Kennett 2003; Reading *et al.* 2003, 2007, 2011). To the east a large-scale portable deployment bracketed the eastern edge of Precambrian outcrop, and contributed a number of sites (Saygin 2007) though strong sedimentary reverberations limited the utility of some results.

Waveform matching techniques using a consistent six-layer gradient and discontinuity model have been favoured, because the gradational Moho in many parts of Australia can be recognized even though the conversions are weak. In such circumstances, stacking methods such as that of Zhu & Kanamori (2000) struggle to extract useful information. In Fig. 4(b) we show estimates of the thickness of the crust–mantle transition based on the full suite of receiver function results. There are many areas where the base of the crust is highly gradational (class W, Fig. 4b) and these match well with interpretations from refraction work, where available.

In recent years Geoscience Australia has significantly augmented the national seismic network and made the data freely available. This new data source has been exploited by Ford *et al.* (2010) who used both *P* and *S* receiver functions to provide depth estimates for both the Moho and deeper discontinuities.

A sequence of dense deployments of three-component shorter period instruments across the southeastern corner of the continent in the WOMBAT project (Rawlinson *et al.* 2011) provides additional information. Despite higher noise levels and more limited bandwidth, valuable receiver function controls on Moho depth can be extracted from teleseismic records using a variety of techniques including stacking, and waveform fitting coupled to local surface wave dispersion results (Tkalčić *et al.* 2011). These higher frequency receiver functions are indicated by squares in the various figures.

Table 1. Table of data sources: RF, receiver functions; HRF, higher frequency receiver functions; Tomo, results from tomographic inversion.

Author	Refraction	RF	HRF	Tomo	Reflection	Map figure
Clitheroe *et al.* (2009)		X				2,6
Collins *et al.* (2003)	X					2,6
Goncharov *et al.* (2007)	X					2,6
Reading & Kennett (2003)		X				6
Reading *et al.* (2003)		X				6
Reading *et al.* (2007)		X				6
Saygin (2007)		X				6
Ford *et al.* (2010)		X				6
Reading *et al.* (2011)		X				6
Tkalčić *et al.* (2011)			X			6
McQueen & Lambeck (1996)				X		6
Rawlinson *et al.* (2011)				X		6
Dooley & Moss (1988)					X	6
This work		X	X		X	6

2.3 Reflection data

An extensive set of information on Moho depth comes from more than 10 000 km of full-crustal reflection profiling carried out across Australia (Fig. 3c). Early short-spread reflection experiments were trialled at a number of sites across Australia in the 1960s (Moss & Dooley 1988). This work was followed by longer reflection profiles conducted using explosive sources from the 1970s to 1997. A nearly 2000 km transect across Southern Queensland was built up in several campaigns in the 1980s. From 1998 reflection profiles have been conducted using powerful vibrator sources. In recent years funding from a number of sources has enabled an expanded programme of data acquisition with over 6500 km of deep reflection profiles carried out since 2004. Finlayson (2010) provides a historical overview and extensive bibliography of the full range of active seismic experiments up to 2006.

The reflection data have not hitherto been used in the compilations of crustal thickness across Australia, except for a few of the point observations reported by Dooley & Moss (1988), indicated by hollow inverted triangles in Fig. 3(c), which were used by Collins *et al.* (2003). We have therefore undertaken a systematic analysis of the full suite of digital record sections held in the national archive at Geoscience Australia, both for explosive sources and vibrator sources, since 1997. For each line the station geometry has been reviewed, and a consistent set of displays have been prepared for each section. When migrated sections are available they have been generally preferred, with cross-checks to the stacked sections in case of ambiguities. In all over 11 000 km of reflection profile have been analysed and Moho picks have been made for nearly all lines.

The Moho pick has been taken at the base of the zone of prominent reflections, with a depth conversion based on the assumption of an rms velocity of 6 km s^{-1} at the base of the crust, since very little control is normally available on the appropriate wave speed profile. Despite this simple approximation, this approach provides crustal thickness estimates that are in good agreement with those obtained from other methods (see Figs 5–7).

We are able to make specific calibrations of this procedure in a number of locations. The long profile across southern Queensland carried out in the 1980s involved both reflection and refraction work and a detailed interpretation is presented by Finlayson (1993). We have compared our depth conversions with these results across a major suite of sedimentary basins. Discrepancies with the refraction results are generally less than 1 km. A similar measure of agreement is found in western Australia between receiver function Moho estimates (Reading *et al.* 2007, 2011) and reflection profiling undertaken in 2010, in this case across the Proterozoic metasediments and Archean outcrop.

The Moho picks have typically been made every 1000 cdp points and thus are mostly at 40 km intervals, but more recently at 20 km intervals. Each pick is accompanied by an assessment of reliability on the scale A–D illustrated in Fig. 4(a). There is considerable variability in the clarity of the base of the reflections. Often the termination is clear, but variations in surface conditions can lead to variability in reflection character even within a single geological domain. In the zones of the thickest crust, the reflections tend to fade away at depth so that the uncertainty in Moho depth can reach 5 km (around 10 per cent); this situation could well be related to mafic underplating of the crust leading to a progressive loss in physical contrasts through the gradational zone.

The reflection profiling provides evidence for a number of sharp changes in Moho depth, notably in central Australia (see, e.g. Goleby *et al.* 1989), where offsets may exceed 20 km. The rate of change of Moho depth can be rapid, with also small jumps (5–8 km) apparently related to crustal sutures as in northern Queensland. Such features pose a challenge when we try to provide a suitable representation of the Moho surface.

2.4 Tomography

Rawlinson *et al.* (2010) have combined refraction results from a marine survey around the island of Tasmania recorded at land stations with teleseismic data recorded at dense seismic arrays. They have developed a high-resolution *P*-wave tomographic model including a description of the crust–mantle boundary. The results tie well with the limited results from reflection work in Tasmania.

We have also used information from a set of linear profiles of portable instruments deployed across the major gravity anomalies in central Australia Lambeck *et al.* (1988). Tomographic inversion of the delay times from distant earthquakes (McQueen & Lambeck 1996) provides good relative control on crustal variations, and on the Arunta line the depth to Moho can be calibrated with reflection seismic results. The same calibration has been applied to the other two profiles.

These two sets of tomographic results are included in Fig. 3(b), alongside the results from receiver functions. The locations of the tomographic sampling is indicated by triangles.

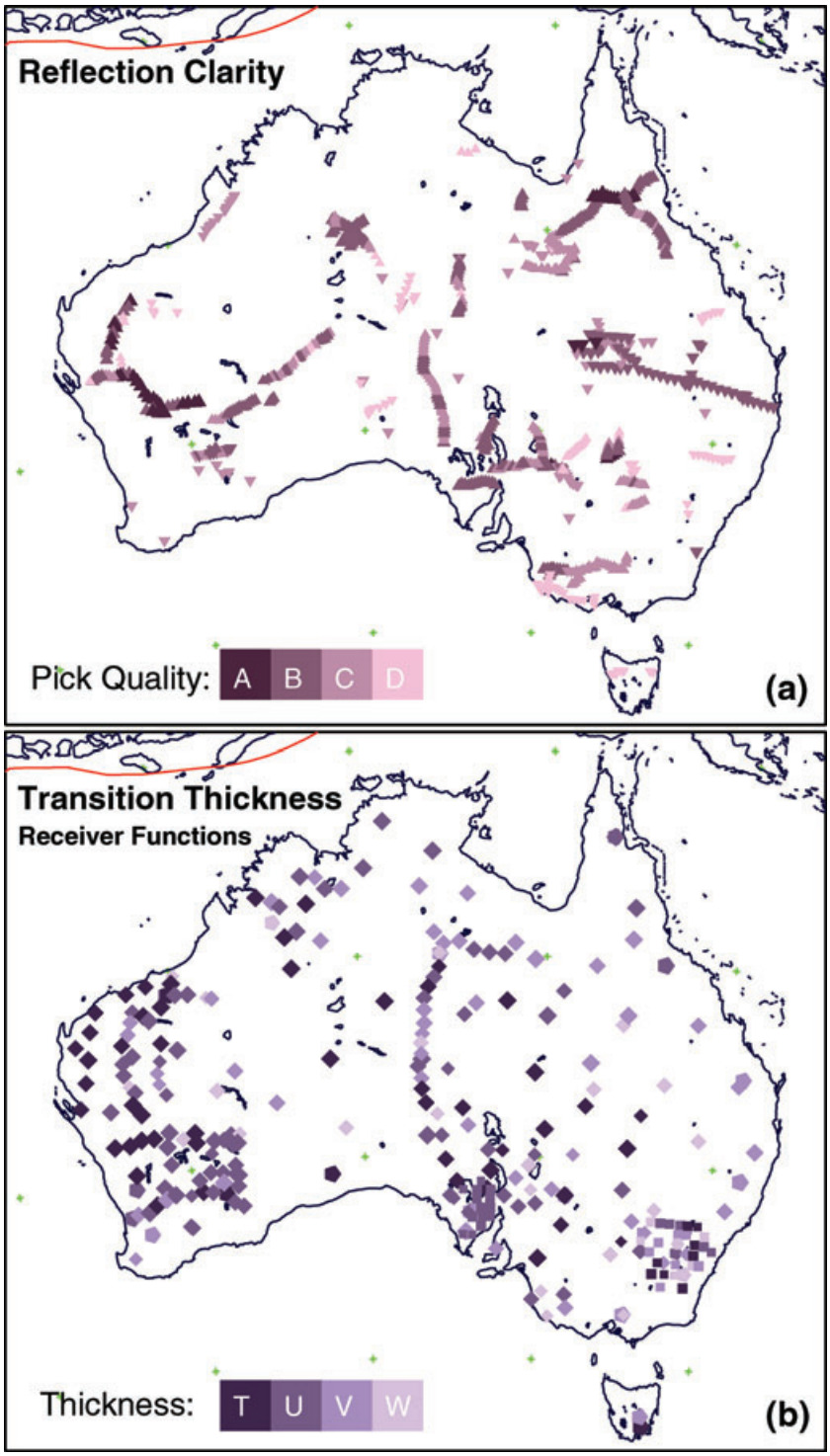

Figure 4. The nature of the Moho from different classes of information: (a) Reflection clarity based on the quality of picking from A—clear, sharp to D—weak, indistinct. (b) Thickness of the crust–mantle transition estimated from receiver function studies, T: < 2 km, U: 2–4 km, V: 4–8 km, W: > 8 km. As in Fig. 3 the size of symbols increases with the reliability of the results.

2.5 A common crust?

The various data sets that we use respond to different aspects of the crust–mantle transition. Refraction techniques have a strong sensitivity to velocity gradients, in both crust and mantle. Receiver function methods exploit conversions between *P* and *S* waves, which are most pronounced for discrete velocity jumps. The conversion from a gradient is muted, with the largest effects associated with the top and bottom of the gradient zone. In reflection profiling we concentrate on the reflectivity patterns, without a direct link to upper-mantle velocities.

In Fig. 4 we summarize the character of the Moho from reflection and receiver function studies. In Fig. 4(a) we display the quality of the pick from the reflection records, where A represents a very clear

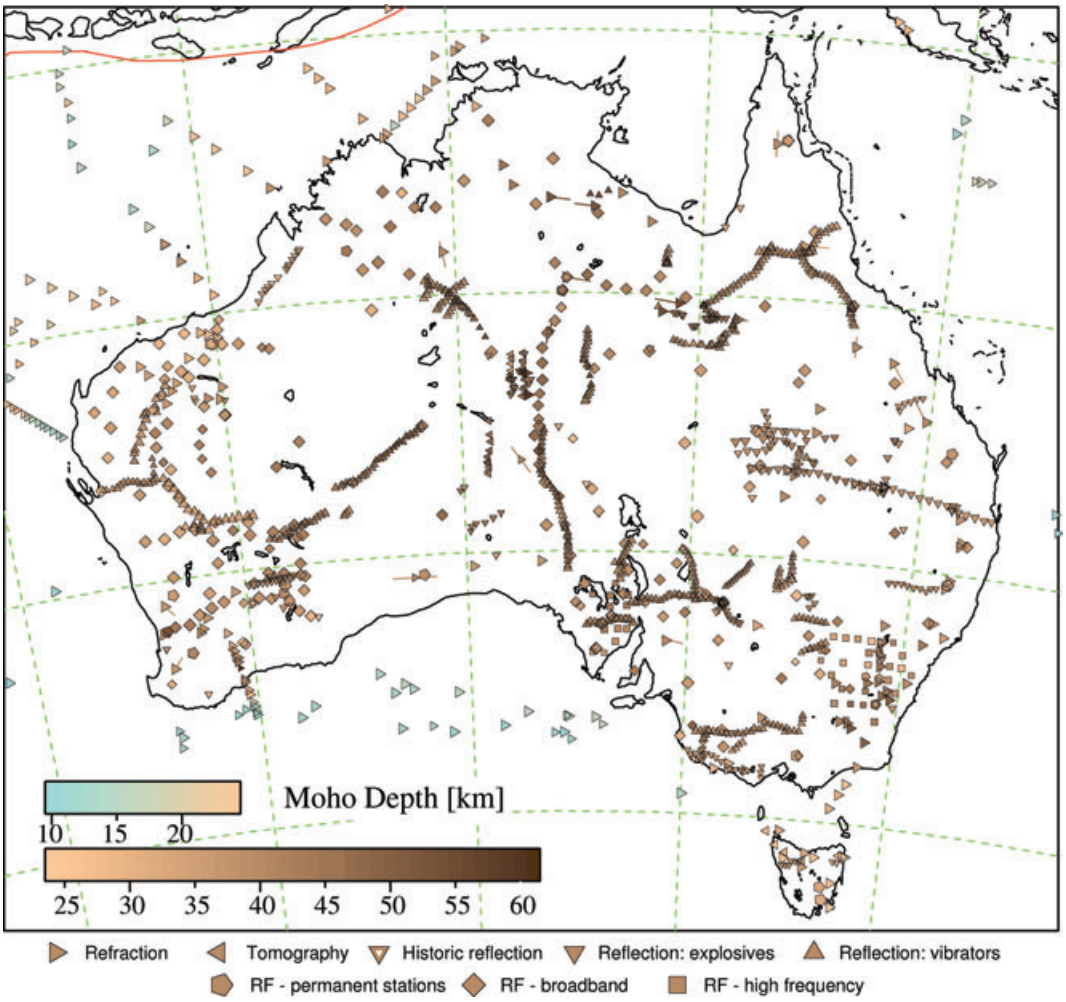

Figure 5. Compilation of all the different styles of Moho estimates with symbol coding by the class of data used. The size of the symbols increases with the reliability of the results. Line segments indicate the sampling from refraction experiments. In general, there is close correspondence between the estimates derived from different techniques (see also Fig. 7).

base of crustal reflections and D either poor record quality, or more commonly a very weak reflection packet with an indistinct base. Fig. 4(b) shows the estimated thickness of the transition between crust and mantle from receiver functions in four categories (T: < 2 km, U: 2–4 km, V: 4–8 km, W: > 8 km). The two different representations of Moho character are generally concordant because a sharp Moho transition will be associated with a very clear reflection, whereas a gradational structure has less marked reflectivity. In each case the size of symbols increases with the reliability of the results.

The full set of Moho depth estimates from the different methods is plotted in Fig. 5, with distinctive symbols for each data type as in Figs 3 and 4. In general, there is a striking level of consistency between the results from the different methods. The few examples of discordant estimates are localized. Although we have plotted the receiver function results at the station location, the distribution of events entering into the construction of the receiver functions is concentrated to the north and east. The sampling at the Moho for the receiver functions will be displaced in these directions, and the subtle shifts (10–20 km horizontally) tend to improve the correspondence between receiver functions and reflection results in central Australia. The symbol sizes in Fig. 5 indicate the relative weights applied to the observations as represented in Table 2.

A number of reflectivity patterns are encountered at the base of the crust along the reflection profiles. The simplest case is a distinct reflector that terminates the crustal reflectivity and, as in parts of western Australia, there is then a close correspondence with the Moho estimates from nearby receiver functions. On occasion we encounter a strong band of reflectivity (up to 3–4 s) at the base of the crust, with a less clear lower boundary. In such circumstances the interface found in receiver function analysis tends to lie at the top of this reflection packet, as in southern central Australia. There is a tendency for the refraction results to lie deeper than other Moho depth estimates in the same area; this is most likely the consequence of the definition of Moho depth we have employed, which will tend to emphasize deep gradients in wave speed.

3 MOHO DEPTH ACROSS THE CONTINENT

Unlike the situation in Europe, where Grad *et al.* (2009) were able to build, in part, on prior detailed maps of Moho depth in part of the European plate, we have constructed our new map of the depth to Moho directly from the set of seismic observations. The new data set (Fig. 5) is both more dense and more heterogeneous in sampling

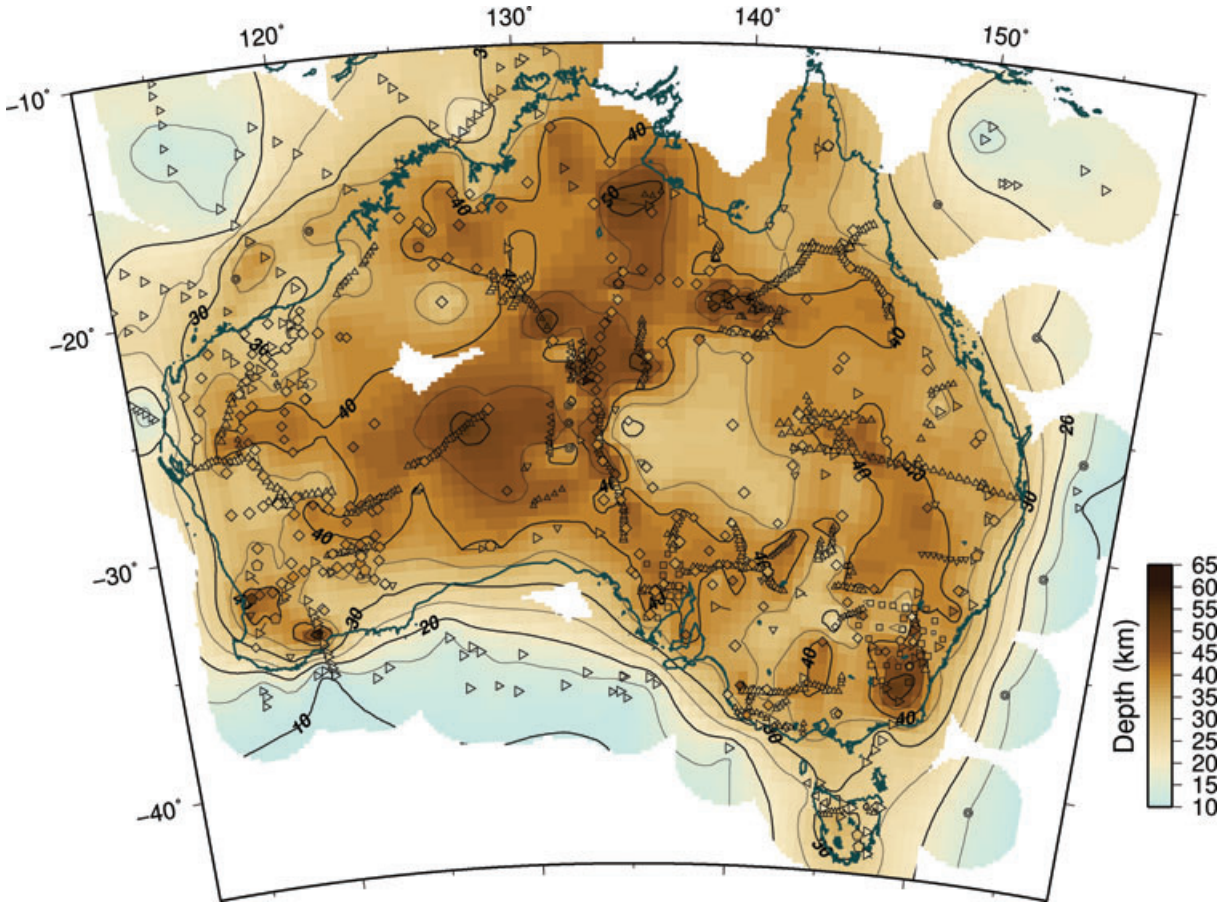

Figure 6. Moho surface constructed from the full set of estimates displayed in Fig. 5. The surface is constructed by interpolating weighted averages for each $0.5^\circ \times 0.5^\circ$ cell, the size of the pixels in the image. The original results are superimposed on the interpolated surface using the same colour coding, shown at the right with depths in kilometres. Additional control points based on the gravity analysis by Aitken (2010) are indicated by double circles; these extra points, applied with low weighting, help define features with strong directionality and constrain, to some extent, the continent–ocean margin to the east of Australia.

than that employed by Collins *et al.* (2003), displayed in Fig. 2. The Moho surface for the new results is shown in Fig. 6; over much of the Australian continent we are able to recognize features with much shorter spatial wavelengths than before, but need to be aware of the holes in coverage linked mostly to desert area with rather limited access. As noted above, the consistency between the Moho depth values derived from very different styles of an analysis is very high across the continent (see Fig. 7). This concordance provides us with considerable confidence in the major patterns in Moho depth. The display of Moho character in Fig. 4 provides a guide to likely errors in the different Moho estimates. Class A, T results will have uncertainties of less than 2 km, whereas Class D, W may reach 5–8 km (about 12–15 per cent of the Moho depth). In most cases the likely errors are less than 10 per cent, and where estimates are available from multiple techniques the Moho depth is much more tightly constrained.

Aitken (2010) has developed an inversion scheme to exploit the gravity field across Australia, in combination with seismic constraints. The primary result of this MoGGIE approach is a map of Moho depth building on the Collins *et al.* (2003) compilation. The constrained inversion of the gravity field also results in the introduction of shorter wavelength features in Moho depth. Indeed there is a strong correspondence between the model presented by Aitken (2010) and the Moho depth patterns from our new seismic compilation. We note the extension of the zone of thickened crust from the north into South Australia with an oblique termination abutting a further zone of thickening in the Gawler Craton, and also the extension of moderately thick crust into the Capricorn Orogen.

As pointed out by Aitken (2010) there is a strong directionality to features in the gravity field, particularly the sequence of strong gravity lows and highs in central Australia with a dominantly east–west orientation. With sparse seismic observations it can be difficult to capture such character in the interpolated maps of Moho depth. Fortunately we have some control in this area from the linear deployments of portable seismometers in central Australia (Lambeck *et al.* 1988).

We have included a limited number of control points from Aitken's (2010) study to improve the rendering of the continental boundary on the eastern margin of the Australian continent, and to capture a significant Moho depression off the northwest coast that is barely sampled by the limited off-shore refraction results. Such gravity-based control points are indicated by double circle symbols on the map of Moho depth thickness in Fig. 6, and are included with low weight.

The interpolated surface of Moho depth is displayed in Fig. 6, with the individual data points superimposed in the colour code associated with their specific data value. As we have already discussed it is not obvious that we should be seeking a smooth Moho surface, and in addition we have to take into account the mild discrepancies between different styles of depth estimates for Moho depth.

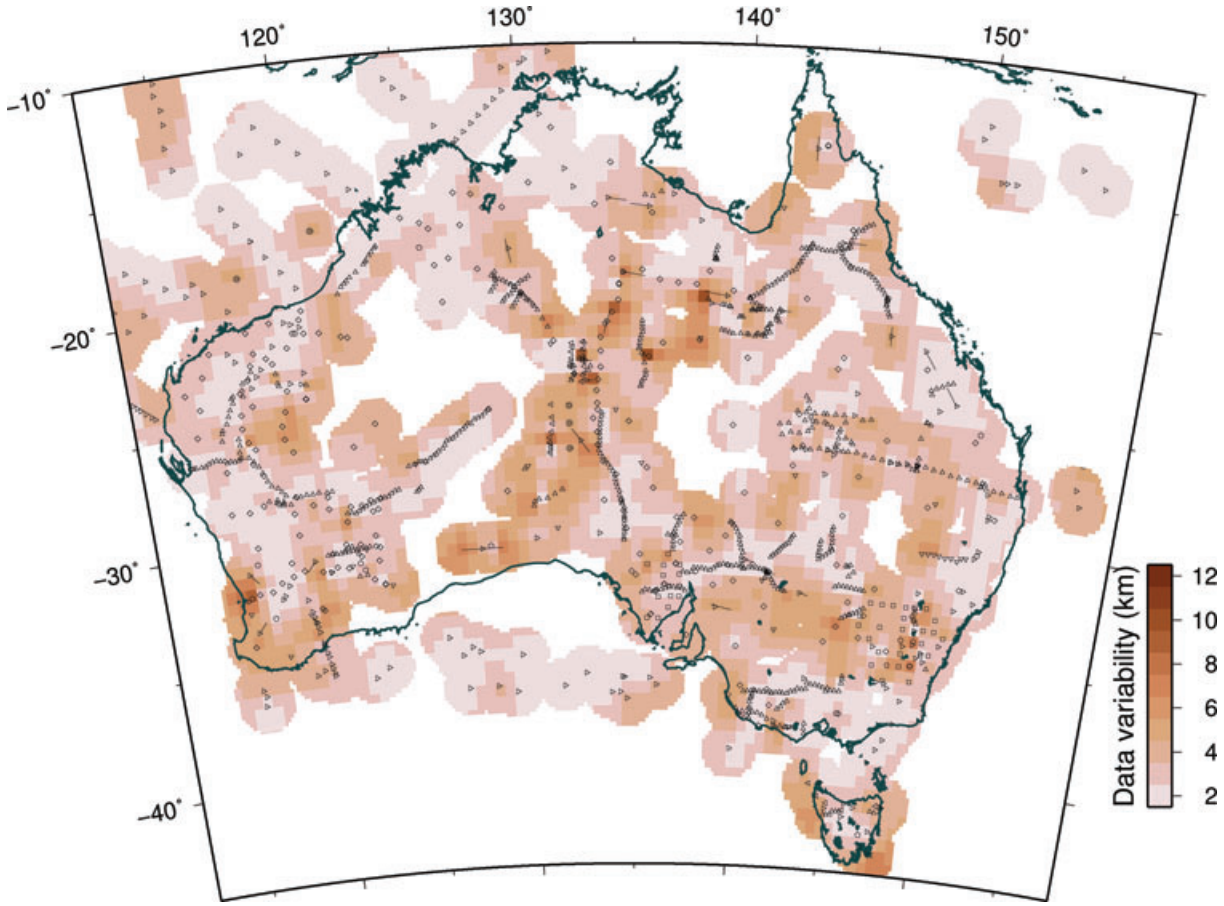

Figure 7. Map of consistency of the Moho depth estimates from the different styles of data displayed in Fig. 5. The influence of the points is allowed to extend to a radius of 125 km. Where multiple estimates occur in a single pixel the weighted standard deviation is plotted. Where there is only a single estimate in a pixel the consistency value is calculated as $12 - 10 \times w$, where w is the weighting applied to the data value (Table 2), a minimum value of 2 km is employed where two values in a pixel agree.

Table 2. Weighting applied to different classes of data.

Data type	Criterion	Weighting			
Refraction		1.0			
Receiver functions	Inversion quality	A: 1.0	B: 0.85	C: 0.70	D: 0.55
Historical reflection		0.8			
Reflection	Pick quality	A: 0.9	B: 0.8	C: 0.7	D: 0.6
Gravity controls		0.5			

The Moho surface in Fig. 6 has been constructed using the interpolation tools from the GMT package (Wessel & Smith 1998) with a conservative approach targeted at 0.5° resolution across the continent. Within each 0.5° × 0.5° cell we take the weighted mean Moho depth from all relevant Moho depth estimates; the weighting of the individual data points is based on the data reliability, as specified in Table 2. The weighted means for each cell are then interpolated using an adjustable tension continuous curvature gridding algorithm (Smith & Wessel 1990). The tension factor is set to 0.45 to allow for steep Moho topography. The resulting surface is displayed allowing the influence of each cellular point to extend no further than 250 km. As can be seen in Fig. 6, we still have regions in the deserts of western Australia where even this generous choice does not provide control on the Moho depth. The error associated with the interpolated surface can be expected to be comparable to that estimated by Clitheroe *et al.* (2009), that is, no more than 2 km where there is good data control and perhaps reaching 5 km in the least well-sampled areas, which are smaller than before.

We have experimented with a number of different representations for the Moho surface, but all have the same fundamental problem that the actual behaviour is not smooth and difficult to represent in summary form. In many ways the data points (Fig. 5) provide the most direct control, but as we have emphasized we have very variable density of information and evidence for considerable local topography on the Moho.

When we compare Fig. 6 with the earlier results displayed in Fig. 2, we see that the main zones of thickened crust are still present, but more fragmented than before, despite the increase in data coverage. There is much greater definition of structure in western and southern Australia. In particular, a very strong gradient in Moho depth is revealed near 135°E, south of 25°S. The combination of receiver function and reflection profiles has dramatically increased the sampling of the Moho across southern central Australia. The configuration of parts of the reflection transects and sites for receiver functions are linked to the main north–south railway and road corridors and lie very close to the edge of the gradient in Moho depth. The sparse points to the east lie in relatively remote outback areas with limited access possibilities.

Fig. 7 shows a measure of the consistency of the different classes of data. Where there are multiple data estimates in an individual pixel we display the weighted standard deviation in kilometres,

using the same weighting as employed in Fig. 6. Elsewhere we use the weights assigned to the data points in the form $12 - 10 \times w$ km, using the weighting w from Table 2, to provide an estimate of reliability of the local Moho depth. A minimum value of 2 km is employed where two depth values in a cell are the same. We have used the same interpolation scheme as in Fig. 6, but now restricted the influence zone of any cell to 125 km. The data points are plotted on the consistency map to provide an indication of the controls on the individual pixels.

The zones with the largest differences between different estimates of Moho depth are nearly all in localities with strong gradients at the base of the crust, such as the Mt Isa block and the Tennant Creek block in northern Australia. The east–west features in central Australia show sharp changes in Moho depth over short distances that map into apparent inconsistency. Rapid changes in Moho depth near the western Australian coast also give a focussed hotspot. There is variability in the Lachlan Fold Belt, but generally refraction and receiver function results are in concordance.

4 DISCUSSION

The patterns of variation in Moho depth show a good general correspondence with the tectonic features of the continent, as noted by Clitheroe *et al.* (2009), but now reinforced by the much increased sampling across the continent. In Fig. 8 we show a simplified map of the basement age across Australia based on geochronological studies. Precambrian basement underlies most of central and western Australia. In the east the situation is more complex, with a broad belt in which there is evidence for ancient basement below Palaeozoic rocks. One scenario that might accommodate this configuration is the accretion of ribbon continents and continental blocks onto the Rodinian breakup edge (e.g. Cayley 2011). Some of these fragments may well have been formed in the process of breakup of Rodinia.

The contours of the interpolated Moho surface from Fig. 6 are superimposed on the basement age in Fig. 8, and show the controls imposed by the major cratonic blocks. Sampling is patchy in the more remote areas of northern Australia and through the Western Deserts, so that we have to be careful in interpreting gradients on the Moho that may be an accident of the disposition of sample points.

Cawood & Korsch (2008) provide a detailed account of the assembly of the main components of central and western Australia during the Proterozoic. The way in which the northern and southern cratons came to their present configuration is still open to debate (*cf.* Betts *et al.* 2002). Following the breakup of the supercontinent Rodinia in the late Proterozoic, the eastern margin of Australia has been reconfigured through accretion of crust in a sequence of orogenies. The Delamarian Orogeny (∼500 Ma) at the craton margin in southern Australia was followed by the Lachlan and New England orogens, bringing arc materials and possible continental ribbons onto the growing eastern margin. The break between Australia and Antarctica and the formation of a failed ocean basin in the Tasman Sea have created the present continent–ocean transitions on the southern and eastern coasts with an often narrow continental shelf.

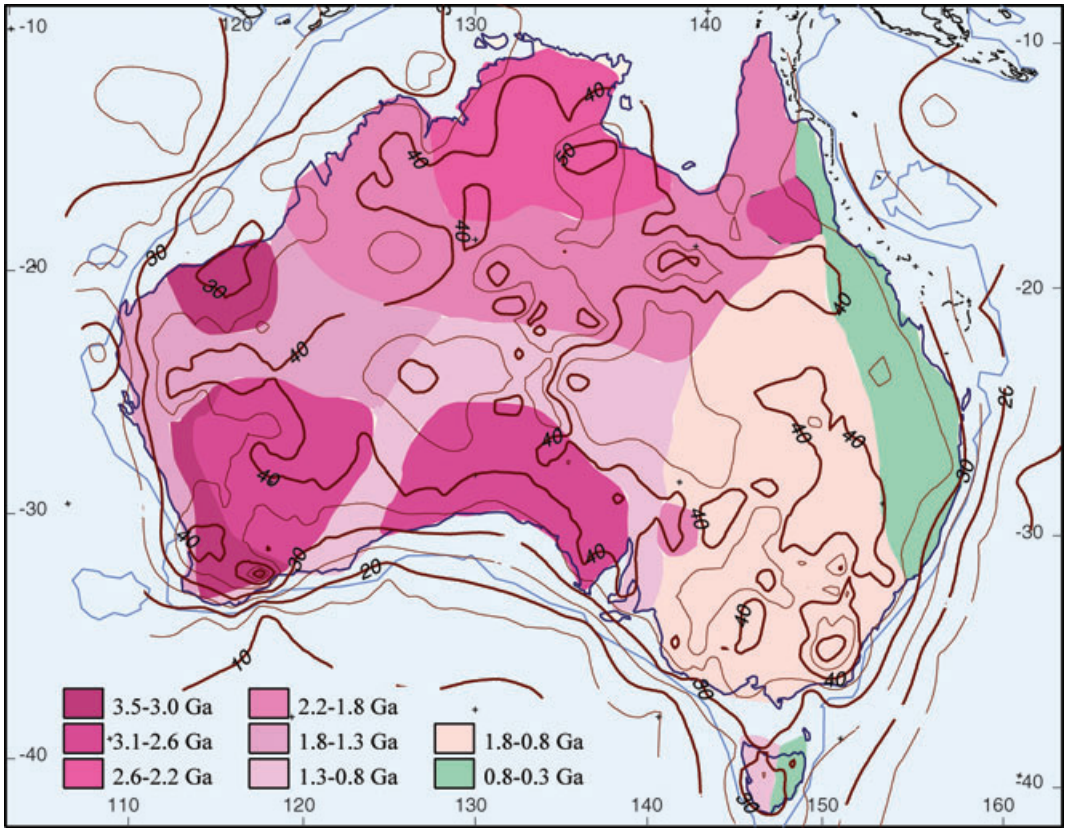

Figure 8. The contours of the interpolated Moho surface, shown in Fig. 6, superimposed on the main age provinces. Much of the thickest crust in west and central Australia is associated with Proterozoic orogens as in the Capricorn Orogen and the Proterozoic complexes in the North Australian Craton. In the east the crustal thickening is linked to the Lachlan Orogen, probably due to mafic underplating.

4.1 Western Australia

The oldest portions of the West Australian craton, the Pilbara craton and the northern Yilgarn craton, have Moho depths in the range 30–35 km. The crust thickens slightly beneath the Neoarchean Hamersley block at the southern edge of the Pilbara, which has extensive banded iron formations, but the main change lies in the Capricorn Orogen where the Moho depth exceeds 40 km. Control in this region is strong from a combination of refraction experiments, receiver functions and recent reflection transects. The thickest crust with a rather indistinct base is found in the Glenburgh terrane at the western edge of the Capricorn Orogen. In the Yilgarn Craton itself, Reading *et al.* (2007) have noted a progression in crustal structure with greater Moho depth associated with younger parts of the craton in the west. This trend can be seen very clearly in Fig. 6. The progression with crustal age in the Archean of western Australia is quite similar to that recently proposed by Thompson *et al.* (2010) for the region around Hudson Bay in Canada.

There is little control on the very narrow strip of the Pinjarra Orogen along the western coastline, just a few receiver functions sit in this zone to the west of the Pilbara. Moho depth appears to be about 30–35 km, with thick sedimentary piles in places.

Sampling of the Moho across the Officer and Eucla basins has only modestly increased since the Collins *et al.* (2003) compilation. Some data of limited quality has been extracted from reflection work. A zone of thickened crust lies to the south of the Musgrave block in the Officer basin, but its linkage to the west is still somewhat uncertain. The near-surface limestones in the Eucla basin provide a barrier to many modes of analysis, but Ford *et al.* (2010) have successfully used *S*-wave receiver functions that are free of near-surface multiples to add a new data point from the permanent seismic station FORT operated by Geoscience Australia.

The results of Aitken (2010) suggest that a Moho depth greater than 40 km may extend across the entire Kimberly block, rather than being truncated as suggested in Figs 6 and 8. Sampling in this region is limited, and the contours in Figs 6 and 8 are influenced by the interaction between onshore and offshore results; whereas the gravity field exploited by Aitken (2010) allows an extension of the results from the centre of the block to the east.

An offshore–onshore refraction experiment into southern western Australia across the Albany-Fraser belt reveals the locally thickened crust, to more than 45 km thick. Unfortunately there is no further seismic control along strike, but the gravity field does not suggest that this feature extends much further east (Aitken 2010). It could however link to the other thicker crust to the west, rather than the saddle suggested by the present interpolation.

4.2 Central Australia

There is generally good control on the major features in the crust through Central Australia from a combination of reflection profiles and receiver function studies, with some major early refraction experiments. The thickest crust in Australia occurs in this region, but the increase in information since the work of Collins *et al.* (2003) indicates that the thickened material is somewhat fragmented. This behaviour is clearly seen on reflection transects, where distinct sharp jumps in the Moho of up to 20 km are associated with the major east–west gravity anomalies (e.g. Goleby *et al.* 1989).

In the north of the Central Australian zone, the crust appears to thin in the Pine Creek Inlier to less than 35 km thick but we have no direct control in the structure in Arnhem Land to the east. In the Proterozoic MacArthur basin, a little further south, refraction and reflection work indicates localized very thick crust. The Tennant Creek block also has crust thickness up to 50 km, but the base of the crust is gradational with an extended gradient from crust into mantle (Bowman & Kennett 1991).

A reflection profile along the Tanami Road from the edge of the Kimberley block towards the heart of Australia, shows a Moho surface close to 40 km for much of its length with a rapid increase in thickness to the south in the Arunta block, where the reflection Moho becomes much less distinct. This would be consistent with a wave speed gradient built up by interleaving of crustal and mantle materials, for example, by underplating.

A prominent feature of the southern zone is the strong gradient in Moho depth close to 135°E that juxtaposes 30 km crust against much thicker material (45 km or more). The area with the thinnest crust is broadly coincident with a topographic low containing the Lake Eyre basin that lies below sea level. The reflection and receiver function coverage of the thicker crust follow the corridor of the main transport routes; access is difficult to the west and so the horizontal extent of the thickened crustal features is not well constrained by the seismic observations, except for the tomographic results from McQueen & Lambeck (1996) in the Musgrave area. Aitken's (2010) study based on gravity analysis suggests that the zones of thickest crust probably extend to about 128°E in the neighbourhood of the north–south Lassiter Shear Zone, a prominent feature in the gravity field.

Although the Gawler Craton in the south, has Archean material, some as old as the Pilbara, the Moho depth is greater than for the older parts of the West Australian cratons. An extensive set of reflection profiles provide good control and it is in this region that we see the largest differences between the results in Figs 6 and 8 and the earlier Moho depth map in Fig. 2. The Curnamona craton now appears as a distinct entity with thicker crust than its surroundings. The eastern side of the Gawler Craton was reworked in the Delamarian Orogen. To the south reflection control indicates crust thicker than 40 km, with a possibly imbricated Moho, but there is insufficient sampling to know whether this is an isolated feature or links back to the thicker crust further to the northwest.

4.3 Eastern Australia

The Mt Isa block has a rather thick crust (greater than 40 km) with quite sharp edges to the south and the northeast. There is a strong gradient zone at the base of the crust and the Moho is only moderately distinct in reflection. On the reflection profile to the Georgetown Inlier, as the crust thins rapidly to around 35 km the reflection Moho becomes very clear. The structures in this area suggest a zone that has been rifted and then recompressed to give the present day configuration. Under the Georgetown Inlier distinct domains of consistent seismic character can be recognized and the transition between domains can be marked by Moho steps, of up to 8 km.

To the south we encounter the thickened crust associated with the Lachlan Orogen, extending under the Eromanga basin. Extensive reflection and refraction work in the 1980s provides good control along 1200 km transect from the interior to the coast. In the southern part of the Lachlan Orogen, the presence of thick crust with a basal crustal gradient was established by refraction experiments. There is now much more information from reflection studies and receiver functions (e.g. Tkalčić *et al.* 2011), and the zone of thicker crust has become more dissected. The high-frequency receiver function studies are more sensitive to discontinuities than gradients and it

is possible that we may pick up an apparent Moho before the true base of the crust. Nevertheless, there is a good tie with the recent reflection profiles. There is only modest seismic control on the New England Orogen but this zone appears to have thinner crust (around 35 km thick) than the Lachlan Fold belt.

5 CONCLUSIONS

By bringing together all the different styles of seismological information for the Australian continent we have been able to create a new map of the Moho surface, with considerably more detail than hitherto. The inclusion of results from the extensive campaigns of reflection profiling has made a major difference, as well as the many receiver functions from the extensive portable seismic deployments across the continent. We are fortunate in having multiple constraints on the Moho in many parts of the country, so that the patterns of Moho depth are generally well controlled. There are still a number of areas where additional sampling would be desirable if logistic considerations permit.

The patterns of Moho depth shown in Figs 6 and 8 do not display any clear dependence on surface or basement age, though as noted by Clitheroe *et al.* (2009, fig. 10) Mesozoic–Cenozoic cover limits the available sampling. The fragmentation of the thickened crust blocks in central Australia and in the Palaeozoic fold belts of the east mean that compared with earlier results we now have a wider range of Moho depths associated with each age province. There is no simple relation between surface age, and what has happened at depth. Indeed some reflection profiles in northern New South Wales display a very clear and coherent Moho around 30 km deep, consistent with receiver function results, yet there is a pattern of complex reflectivity in the mantle beneath suggesting tectonic processes extending below the current crust.

As we have added more data we see much shorter scale features in the depth to Moho. Steps in the Moho associated with the Palaeozoic Alice Springs Orogeny in central Australia had been recognized from gravity and reflection work (e.g. Goleby *et al.* 1989), but there are a number of other smaller Moho steps revealed by reflection profiling.

The compilation of Moho depths and the Moho surface can be viewed and downloaded from the website: http://rses.anu.edu.au/seismology/AuSREM/AusMoho, and updates of the information will be made as new data becomes available. We aim to supplement this Moho compilation with a full synthesis of all available results on the Australian crust to produce a full 3-D model for the continent.

ACKNOWLEDGMENTS

Funding support for the passive seismic work has been provided from the Australian National University, from Discovery Projects funded by the Australian Research Council, from the Predictive Mineral Discovery Cooperative Research Centre, and the AuScope infrastructure initiative. The active seismic work was initiated by the Bureau of Mineral Resources (subsequently Australian Geological Survey Organisation and now Geoscience Australia). The recent surveys have been funded through the Australian Government Onshore Energy Security Program, the AuScope infrastructure initiative and State investments from Queensland, Western Australia, South Australia, New South Wales and Victoria.

REFERENCES

Aitken, A.R.A., 2010. Moho geometry gravity inversion experiment (MoGGIE): a refined model of the Australian Moho and its tectonic and isostatic implications, *Earth planet. Sci. Lett.,* **297,** 71–83.

Betts, P.G., Giles, D., Lister, G.S. & Frick, L.R., 2002. Evolution of the Australian Lithosphere, *Austral. J. Earth Sci.,* **49,** 661–692.

Bowman, J.R. & Kennett, B.L.N., 1991. Propagation of *Lg* waves in the North Australian craton: influence of crustal velocity gradients, *Bull. seism. Soc. Am.,* **81,** 592–610.

Cawood, P. & Korsch, R.J., 2008. Assembling Australia: proterozoic building of a continent, *Precambrian Res.,* **166,** 1–38.

Cayley, R., 2011. Exotic crustal block accretion to the eastern Gondwanaland margin in the late Cambrian, Tasmania, the Selwyn Block, and implications for the Cambrian-Silurian evolution of the Ross, Delamarian and Lachlan orogens, *Gondwana Res.,* **19,** 628–649.

Clitheroe, G., Gudmundsson, O. & Kennett, B.L.N., 2009. The crustal thickness of Australia, *J. geophys. Res.,* **105,** 13 697–13 713.

Collins, C.D.N., 1991. The nature of the crust-mantle boundary under Australia from seismic evidence, in *The Australian Lithosphere,* Vol. 17, pp. 67–80. ed. Drummond, B.J., Spec. Publ., Geol. Soc. Aust.

Collins, C.D.N., Drummond, B.J. & Nicoll, M.G., 2003. Moho depth patterns in the Australian continent, in *The Evolution and Dynamics of the Australian Plate,* pp. 121–128, eds Müller, D. & Hillis, R., Geological Society of Australia Special Publication, Vol. 22 and Geological Society of America Special Paper 372.

Direen, N.G. & Crawford, A.J., 2003. The Tasman Line: where is it, what is it, and is it Australia's Rodinian breakup boundary? *Austral. J. Earth Sci.,* **50,** 491–502.

Dooley, J.C. & Moss, F.J., 1988. Deep crustal reflections in Australia 1957-1973 – II. Crustal models, *Geophys. J. R. astr. Soc.,* **293,** 239–249.

Finlayson, D.M., 1993. Crustal architecture across the Phanerozoic Australia along the Eromanga-Brisbane Geoscience Transect: evolution and analogues, *Tectonophysics,* **219,** 191–211.

Finlayson, D.M., 2010. *A Chronicle of Deep Seismic Profiling across the Australian Continent and its Margins, 1946-2006,* D.M. Finlayson, Canberra, pp 255. Available from: doug.finlayson@netspeed.com.au.

Fishwick, S., Heintz, M., Kennett, B.L.N., Reading, A.M. & Yoshizawa, K., 2008. Steps in lithospheric thickness within eastern Australia, evidence from surface wave tomography, *Tectonics,* **27,** TC0049, doi:10.129/2007TC002116.

Ford, H.A., Fischer, K.M., Abt, D.L., Rychert, C.A. & Elkins-Tanton, L.T., 2010. The lithosphere–asthenosphere boundary and cratonic lithospheric layering beneath Australia from *Sp* wave imaging, *Earth planet. Sci. Lett.,* **300,** 299–310.

Goleby, B.R., Shaw, R.S., Wright, C., Kennett, B.L.N. & Lambeck, K., 1989. Geophysical evidence for 'thick-skinned' crustal deformation in central Australia, *Nature,* **337,** 325–330.

Goncharov, A., Deighton, I., Tischer, M. & Collins, C., 2007. Moho depth in Australia: where, how and what for? *ASEG Extended Abstracts*, Perth, Western Australia.

Grad, M., Tiira, T. & ESC Working Group, 2009. The Moho depth map of the European Plate, *Geophys. J. Int.,* **176,** 279–292.

van der Hilst, R., Kennett, B.L.N., Christie, D. & Grant, J., 1994. Project SKIPPY explores the lithosphere and mantle beneath Australia, *EOS, Trans. Am. geophys. Un..,* **75,** 177.

Kennett, B.L.N., 2003, Seismic Structure in the mantle beneath Australia, in *The Evolution and Dynamics of the Australian Plate,* eds Müller, D. & Hillis, R., pp. 7–23, Geological Society of Australia Special Publication, Vol. 22, and Geological Society of America Special Paper 372.

Kennett, B.L.N., Fishwick, S., Reading, A.M. & Rawlinson, N., 2004. Contrasts in mantle structure beneath Australia – relation to Tasman Lines? *Austral, J. Earth Sci.,* **51,** 563–569.

Lambeck, K., Burgess, G. & Shaw, R.D., 1988. Teleseismic travel-time anomalies and deep crustal structure in central Australia, *Geophys. J. R. astr. Soc.,* **94,** 105–124.

McQueen, H.W.S. & Lambeck, K., 1996. Determination of crustal structure in central Australia by inversion of traveltime residuals, *Geophys. J. Int.,* **126,** 645–662.

Mohorovičić, A., 1910. Das beben von 8 Okt. 1909, *Jahrb. Meteorol. Obs. Agram (Zagreb),* **9,** Teil IV.

Moss, F.J. & Dooley, J.C., 1988. Deep crustal reflection recordings in Australia 1957-1973 – I. Data acquisition and presentation, *Geophys. J. R. astr. Soc.,* **293,** 229–238.

O'Reilly, S.Y. & Griffin, W.L., 1996. 4-D Lithosphere mapping: Methodology and examples, *Tectonophysics,* **262,** 3–18.

Rawlinson, N., Tkalčić, H. & Reading, A.M., 2010. Structure of the Tasmanian lithosphere from 3D seismic tomography, *Austral. J. Earth Sci.,* **57,** 381–394.

Rawlinson, N., Kennett, B.L.N., Vanacore, E., Glen, R.A. & Fishwick, S., 2011. The structure of the upper mantle beneath the Delamerian and Lachlan orogens from simultaneous inversion of multiple teleseismic datasets, *Gondwana Res.,* **20,** doi:10.1016/j.gr.2010.11.001.

Reading, A.M. & Kennett, B.L.N., 2003. Lithospheric structure of the Pilbara Craton, Capricorn Orogen and northern Yilgarn Craton, Western Australia, from teleseismic receiver functions, *Austral. J. Earth Sci.,* **50,** 439–445.

Reading, A.M., Kennett, B.L.N. & Dentith, M.C., 2003. The seismic structure of the Yilgarn Craton, Western Australia, *Austral. J. Earth Sci.,* **50,** 427–438.

Reading, A.M., Kennett, B.L.N. & Goleby, B., 2007. New constraints on the seismic structure of West Australia: evidence for terrane stabilization prior to the assembly of an ancient continent? *Geology,* **35,** 379–379.

Reading, A.M., Tkalčić, H. & Kennett, B.L.N., 2011. Seismic structure of the crust and uppermost mantle of the Capricorn and Paterson Orogens and adjacent cratons, Western Australia, from passive seismic experiments, *Precambrian Res.,* doi:10.1016/precamres.2011.07.001.

Sambridge, M.S., 1999. Geophysical inversion with a neighbourhood algorithm – I. Searching a parameter space, *Geophys. J. Int.,* **138,** 479–494.

Saygin, E., 2007. Seismic receiver and noise correlation based studies in Australia, *Ph.D. thesis*, The Australian National University.

Shibutani, T., Sambridge, M. & Kennett, B., 1996. Genetic algorithm inversion for receiver functions with application to crust and uppermost mantle structure beneath eastern Australia, *Geophys. Res. Lett.,* **23,** 1829–1829.

Smith, W.H.F. & Wessel, P., 1990. Gridding with continuous curvature splines in tension, *Geophysics,* **55,** 293–305.

Thompson, D.A., Bastow, A.D., Helffrich, G., Kendall, J.-M., Wookey, J., Snyder, D.B. & Eaton, D.W., 2010. Precambrian crustal evolution: seismic constraints from the Canadian Shield, *Earth planet. Sci. Lett.,* **297,** 655–666.

Tkalčić, H., Rawlinson, N., Arroucau, P., Kumar, A. & Kennett, B.L.N., 2011. Multi-step modelling of receiver-based seismic and ambient noise data from WOMBAT array: crustal structure beneath southeast Australia, *Geophys. J. Int.,* submitted.

Wessel, P. & Smith, W.H.F., 1998. New, improved version of generic mapping tools released, *EOS, Trans. Am. geophys. Un.,* **79,** 579.

Zhu, L. & Kanamori, H., 2000. Moho depth variation in southern California from teleseismic receiver functions, *J. geophys. Res.,* **105,** 2969–2980.

SUPPORTING INFORMATION

Additional Supporting Information may be found in the online version of this article:

Figures. Large format versions of Figs 2, 5 and 6 are provided in the supplement.

Please note: Wiley-Blackwell are not responsible for the content or functionality of any supporting materials supplied by the authors. Any queries (other than missing material) should be directed to the corresponding author for the article.